A Comparison of CIELAB and CIECAM97s

Nathan Moroney
Hewlett-Packard Laboratories
Palo Alto, California, USA

Abstract

The recently developed CIE color appearance model, CIECAM97s, provides an extension of the previously recommended CIE color spaces. This paper examines the new color appearance model by comparing it to CIELAB, one of the more widely used color spaces for digital color imaging. First, the perceptual attributes common to both spaces are compared and contrasted. Second, examining device gamuts in CIELAB and CIECAM97s further highlights differences in the spaces. Lastly, the trends in the color differences for the two color spaces are assessed. The focus of this paper is to highlight differences using simple numeric calculations.

Introduction

The CIELAB color space was introduced in 1976 to provide a more perceptually uniform color space in which to compute color differences.[1] The CIECAM97s color appearance model was proposed in 1997 to model a subset of color appearance phenomena.[2] To better understand both color spaces, it is useful to look at the input and output parameters, as well as a general flowchart for CIECAM97s.

Both color spaces use sample and white point tristimulus values as input parameters but CIECAM97s has several additional input parameters. The added input parameters for CIECAM97s are surround, luminance of the adapting field and the luminance of the background. The two color spaces have perceptual correlates for lightness, chroma and hue but once again CIECAM97s has several additional output parameters. The perceptual attributes of brightness, colorfulness, saturation and hue quadrature can be computed using CIECAM97s. The similarities and differences between the two spaces are shown in Figure 1.

The CIELAB perceptual attributes are computed using a Von Kries type transformation followed by a non-linear scaling. The Von Kries transformation is applied directly to the tristimulus values of the sample and the perceptual attributes are lightness, chroma and hue. These attributes are computed by converting the rectangular form of CIELAB to cylindrical coordinates.

The CIECAM97s computations are more complex, as can be seen in the flowchart shown in Figure 2. Two cone fundamental spaces are used in the model. The modified Von Kries is performed in the Bradford cone space[3] while the perceptual attributes are computed using the Hunt-Pointer-Estevez cone space. Furthermore, note the parallel branch processing the white point, using the perceptual attributes of the white for computing the sample attributes. The luminance of the test adapting field is used in multiple places in the calculations. The other input parameters, such as luminance of the background and the surround, are used only while calculating the output attributes given the post adaptation compressed cone responses.[4]

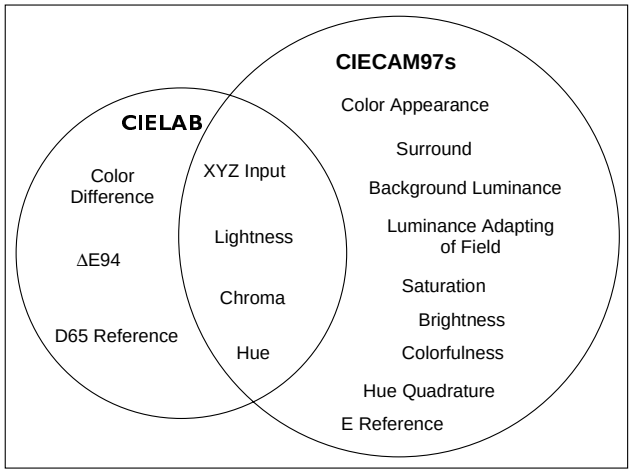

Figure 1. Selected similarities and differences between CIELAB and CIECAM97s

One subtle, yet significant, difference between the two spaces is the order of computing the perceptual attributes. Chroma and hue are computed from the CIELAB a* and b* opponent axes using the geometric transform to convert from Cartesian to polar coordinates. In contrast, a preliminary rectangular coordinate system is used to compute CIECAM97s chroma and hue. Then the chroma and hue are converted back to rectangular coordinates using a polar to Cartesian geometric transformation.

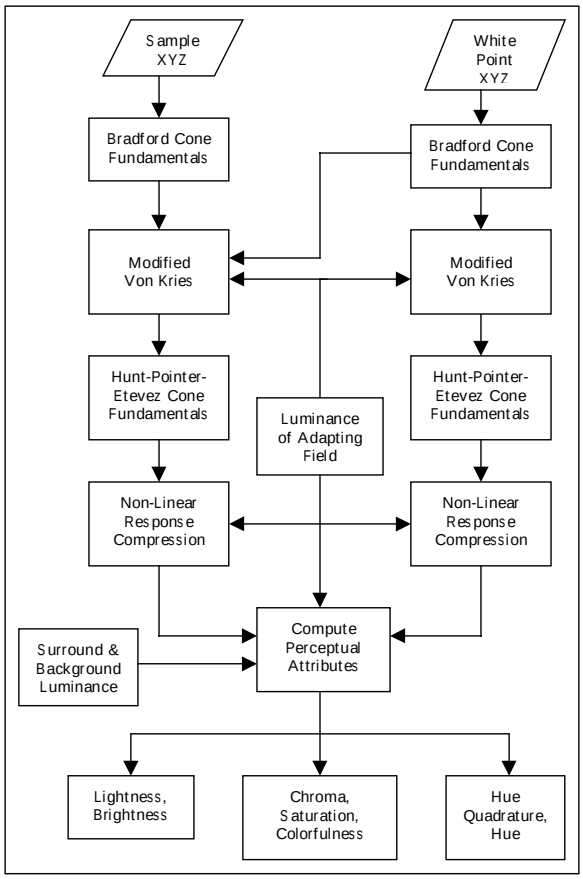

Figure 2. A simplified CIECAM97s flowchart

The CIECAM97s color appearance model offers a potential mechanism for a viewing condition independent color representation by modeling several color appearance phenomena. Therefore CIECAM97s could be used to replace CIELAB as a color interchange space.

Correlating Perceptual Attributes

The CIELAB and CIECAM97s perceptual attributes of lightness, chroma and hue are graphically compared in Figures 3 to 5 for a subset of viewing conditions. The average surround viewing conditions were based on the ΔE_{94} recommendations[5] of 1000 lux under D65 with Y_b set to 20. The D65 white point and Y_b of 20 was used for all of the other viewing conditions. The dim and dark L_a value was set to 80 and the cut sheet L_a was set to 500.

The curves shown in Figure 3 were derived by starting with a neutral L* ramp going from 0 to 100 and computing the corresponding tristimulus values using a D65 white point. These tristimulus values were then converted to the corresponding CIECAM97s coordinates using the viewing conditions described previously. The original CIELAB lightness or L* is shown on the x-axis and the resulting CIECAM97s lightness or J is shown on the y-axis. The variable black point has been plotted for other surround corrections[6] but it is interesting to note the range and order for the black points in CIECAM97s and other models. In contrast, Bartelson's L** is nearly zero for all surrounds when the sample is zero lumiance.[7]

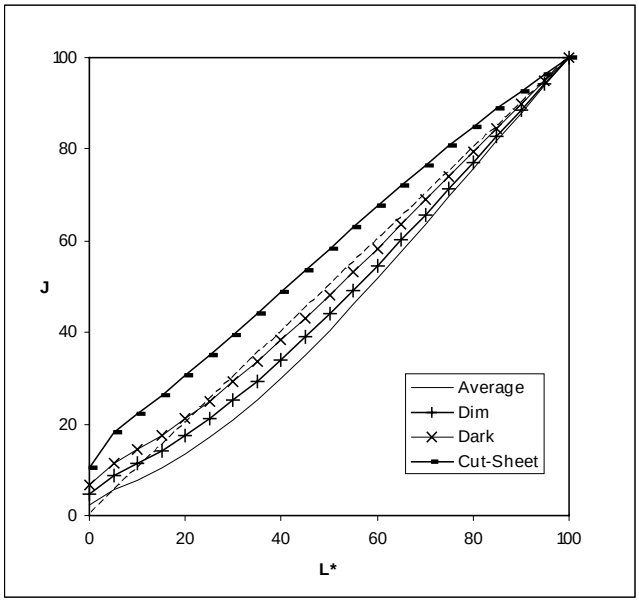

Figure 3. Comparison of L and J based on a neutral ramp generated in CIELAB using a D65 white point.*

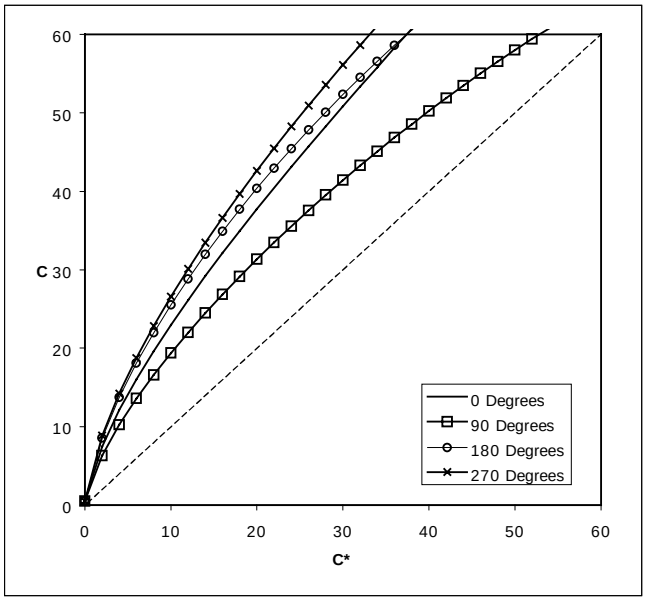

Figure 4. Comparison of C and C based on chroma ramps every 90 degrees generated in CIELAB using a D65 white point.*

CIELAB chroma or C* and CIECAM97s chroma or C are compared in Figure 4. This data was derived by creating C* ramps from 0 to 70 every 90 degrees at an L* of 50. The resulting LCh data was then converted to tristimulus values using a D65 white point and then converted to CIECAM97s JCh space using the average viewing condition described earlier. The x-axis is CIELAB chroma and the y-axis is

CIECAM97s chroma. All of the curves show a significant degree of expansion, with yellow being expanded the least. At higher chroma levels, the CIECAM97s chroma begins to become compressed for some hue angles.

The hue angles of the two spaces are compared in Figure 5. This plot was generated by creating chroma ramps from 0 to 100 every 45 degrees at a constant L* of 50. These LCh ramps were converted to CIECAM97s JCh coordinates using D65 and the previously defined average viewing condition. The JCh data was then converted to Cartesian coordinates using standard trigonometric transforms. The x-axis is a red-green abscissa and the y-axis is a yellow-blue ordinate. There is a drastic difference in the blue hue angles at higher chromas. There are also smaller differences at other hue angles and minimal differences for reds and greens.

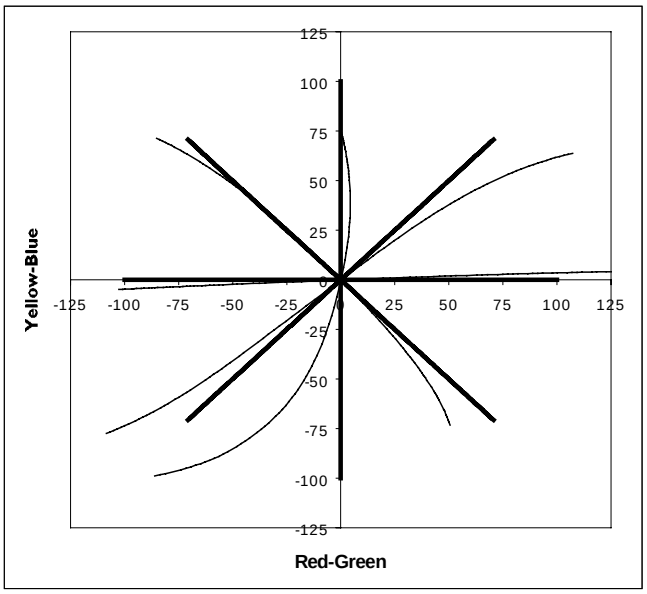

Figure 5. CIELAB chroma ramps, shown as bold lines, every 45 degrees at an L of 50 converted to CIECAM97s, shown as thin lines, using D65 and average surround.*

The results shown in Figures 3 to 5 demonstrate significant differences between CIELAB and CIECAM97s. Limited testing of other viewing conditions, L* levels and sampling schemes show similar results. The noteworthy differences include a variable black point, overall chroma expansion and a significant redefinition of the blue hue angles.

Gamut Processing

The underlying structure of both spaces can also be compared by rendering the same gamut in both CIELAB and CIECAM97s. This was done for the sRGB[8] gamut and the results are shown in Figures 6 and 7. The sRGB specification was used to compute tristimulus values that were then converted to CIELAB and CIECAM97s coordinates. The CIECAM97s viewing conditions were set to dim surround with La of 80 and a D65 white point. The JCh values were converted to rectangular coordinates using the following equations:

$$a_{c97} = C * cos(h) \quad (1)$$

$$b_{c97} = C * sin(h) \quad (2)$$

The subscript, C97, in equations 1 and 2 indicate that the rectangular coordinates are not a and b, the preliminary coordinates and are based on chroma as opposed to saturation, which would be noted a_{S97} and b_{S97}.

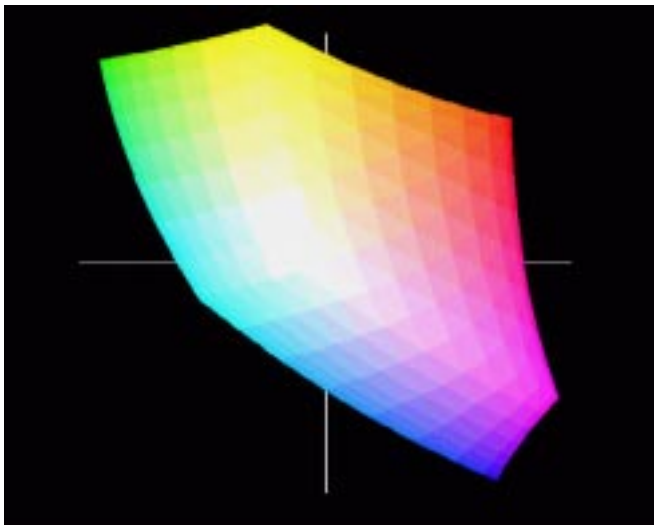

Figure 6. The sRGB gamut looking down L on the white pole in the CIELAB color space.*

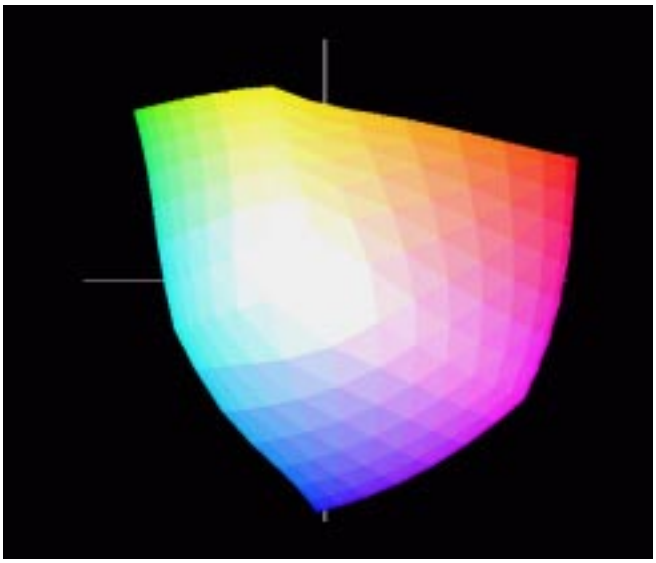

Figure 7. The sRGB gamut looking down J on the white pole in the CIECAM97s color space with a dim surround.

The gamuts shown in Figures 6 and 7 further demonstrates the significant shift in the blues in the CIECAM97s color space. The blue hue linearity has been

shown to be a problem for CIELAB.[9] The results shown in Figures 5 and 7, indicate possible improvements in CIECAM97s blue hue linearity. Initial visual evaluations have also shown blue to lighter gray gradients to be especially sensitive to the differences in blue hues. These diagonal projections, similar to some out-of-gamut mapping algorithms, may be a more difficult test than projections at a constant lightness[10] or to the gamut white or black.

The sRGB gamuts also show that the CIECAM97s space is more curved and irregular. To illustrate, using the eight corners of the cube to compute the gamut volume results in a –10% error for CIELAB and –30% error for CIECAM97s. This impacts issues such as comparing, encoding and processing device gamuts.

A final issue relating to gamut volume is the relative size of the gamut volumes as a function of surround. Although not extensively researched, the perceptual gamut volumes[11] might be expected to rank average, dim and dark surround in order of decreasing size. However, using the sRGB gamut the ranking from largest to smallest is dim, average and then dark. The average surround perceptual gamut is approximately 90% of the dim surround gamut and the dark surround perceptual gamut is about 65% of the dim surround gamut.

Color Differences

To compare color differences, a numeric simulation was done using sRGB. First, color differences within one viewing condition were computed by comparing sRGB using a gamma of 1.8 versus 2.4. Second, the color differences across two viewing conditions were computed with sRGB with a D65 white point and with a D90 white point. The CIECAM97s color differences were computed using a simple three-dimensional Euclidean distance:

$$\Delta E_{97} = (\Delta J^2 + \Delta a_{C97}^2 + \Delta b_{C97}^2)^{1/2} \qquad (3)$$

where a_{C97} and b_{C97} are the rectangular coordinates calculated using equations 1 and 2.

Table 1. Color differences using a gamma of 1.8 versus 2.4 for sRGB computations.

Metric	Average	Maximum
ΔE^*_{ab}	9.9	20.5
ΔE_{94}	6.1	12.2
ΔE_{97}	9.9	19.0

The results shown in Table 1 list the average and maximum of 125 CIELAB, ΔE_{94} and CIECAM97s color differences. The magnitude of the CIECAM97s color differences agrees more closely with CIELAB than with ΔE_{94}. A linear least squares fit of the CIECAM97s color differences has an R^2 of 0.61 using CIELAB and 0.37 using ΔE_{94}. This indicates that there is a rough agreement of CIELAB and CIECAM97s within one viewing condition, although for large color differences[12] it would be better to have a higher correlation with ΔE_{94}.

Table 2. Color differences using a white point of D90 versus D65 for sRGB computations.

Metric	Average	Maximum
ΔE^*_{ab}	3.9	9.2
ΔE_{94}	1.8	4.4
ΔE_{97}	11.7	20.6

The average and maximum color differences are again listed for D90 versus D65 sRGB in Table 2. This corresponds to a comparison of two viewing conditions. In this case, the CIECAM97s color differences are an order of magnitude large than the ΔE_{94} differences and roughly a factor of 2 larger than CIELAB. This demonstrates that CIECAM97s is more sensitive to changes in viewing conditions than either ΔE_{94} or CIELAB. In fact, it is interesting to note that CIECAM97s is the only color difference metric to find the color differences resulting from a change in white point comparable to the color differences resulting from a change in gamma.

Conclusions

CIECAM97s is clearly an extension of the basic chromatic adaptation model and perceptual attributes of CIELAB. However, CIELAB and CIECAM97s differ with respect to black encoding, chroma and blue hue angles. The hue differences in blue are a potential improvement over CIELAB. The CIECAM97s color space is also a more complex space for gamut rendering and processing. In addition, the maximum CIECAM97s perceptual gamut volume can occur using the dim surround, although it is not clear how to interpret this finding. Finally, the CIECAM97s color differences are similar in magnitude and roughly correlated to ΔE^*_{ab} for color differences within one viewing condition. In comparison, the CIECAM97s color differences are more than twice as large as the CIELAB color differences across viewing conditions, for example a change in white point.

References

1. *Colorimetry*, 2nd Ed., CIE Publ. No. 15.2, Central Bureau of the CIE, Vienna, (1986).
2. R.W.G. Hunt, "The Function, Evolution and Future of Colour Appearance Models", Proc. CIE Expert Symposium '96 on Colour Standards for Image Technology, CIE x010-1996, pp. 41-45, (1996).
3. Paul M. Hubel and Graham Finlayson, "Sharp Transformations for Color Appearance", *Proc. Color Imaging: Device Independent Color, Color Hardcopy, and Graphic Arts III*, **3300**, 159-164 (1998).
4. M.R. Luo and R.W.G. Hunt, "The Structure of the CIE

1997 Colour Appearance Model (CIECAM97s)", *Col. Res. & App*, **23**, 138-146, (1998).
5. Klaus Witt, "CIE Guidelines for Coordinated Future Work on Industrial Color Difference Evaluation", *Col. Res. & Appl*., **22**, pp. 298-307 (1995).
6. Mark D. Fairchild, "Considering the Surround in Device-Independent Color Imaging", *Col. Res & Appl*., **20**, pp. 352-363 (1995).
7. C. J. Bartelson, "Optimum Image Tone Reproduction", *J. of SMPTE*, **84**, pp. 613-618 (1975).
8. International Electrotechnical Commission, "Default RGB Colour Space- sRGB", 3rd Working Draft of IEC 61966-2.1, Jan. 1, (1998).
9. Po-Chieh Hung and Roy S. Berns, "Determination of Constant Hue Loci for a CRT Gamut and Their Predictions Using Color Appearance Spaces", *Col. Res. & Appl*., **20**, pp 285-295, (1995).
10. Fritz Ebner and Mark D. Fairchild, "Finding constant hue surfaces in color space", *Proc. Color Imaging: Device Independent Color, Color Hardcopy, and Graphic Arts III*, **3300**, 107-117, (1998).
11. Mark D. Fairchild, *Color Appearance Models*, Addison Wesley, Reading, Massachusetts, (1998).
12. M.R. Pointer and G.G. Attridge, "Some Aspects of the Visual scaling of Large Color Differences", *Col. Res. & Appl*., **22**, 298-307, (1997).